BIOCHEMISTRY
including biophysical chemistry & molecular biology

Article

pubs.acs.org/biochemistry

Comparative Hydrogen–Deuterium Exchange for a Mesophilic vs Thermophilic Dihydrofolate Reductase at 25 °C: Identification of a Single Active Site Region with Enhanced Flexibility in the Mesophilic Protein

Olayinka A. Oyeyemi,[†] Kevin M. Sours,[‡] Thomas Lee,[‡] Amnon Kohen,[∥] Katheryn A. Resing,[‡,⊥] Natalie G. Ahn,*[,‡,§] and Judith P. Klinman*[,†]

[†]Department of Chemistry, Department of Molecular and Cell Biology, and the California Institute for Quantitative Biosciences (QB3), University of California, Berkeley, Berkeley, California 94720, United States

[‡]Department of Chemistry and Biochemistry, University of Colorado, Boulder, Colorado 80309, United States

[§]Howard Hughes Medical Institute, University of Colorado, Boulder, Colorado 80309, United States

[∥]Department of Chemistry, The University of Iowa, Iowa City, Iowa 52242, United States

Supporting Information

ABSTRACT: The technique of hydrogen–deuterium exchange coupled to mass spectrometry (HDX-MS) has been applied to a mesophilic (*E. coli*) dihydrofolate reductase under conditions that allow direct comparison to a thermophilic (*B. stearothermophilus*) ortholog, *Ec*-DHFR and *Bs*-DHFR, respectively. The analysis of hydrogen–deuterium exchange patterns within proteolytically derived peptides allows spatial resolution, while requiring a series of controls to compare orthologous proteins with only ca. 40% sequence identity. These controls include the determination of primary structure effects on intrinsic rate constants for HDX as well as the use of existing 3-dimensional structures to evaluate the distance of each backbone amide hydrogen to the protein surface. Only a single peptide from the *Ec*-DHFR is found to be substantially more flexible than the *Bs*-DHFR at 25 °C in a region located within the protein interior at the intersection of the cofactor and substrate-binding sites. The surrounding regions of the enzyme are either unchanged or more flexible in the thermophilic DHFR from *B. stearothermophilus*. The region with increased flexibility in *Ec*-DHFR corresponds to one of two regions previously proposed to control the enthalpic barrier for hydride transfer in *Bs*-DHFR [Oyeyemi et al. (2010) *Proc. Natl. Acad. Sci. U.S.A. 107*, 10074].

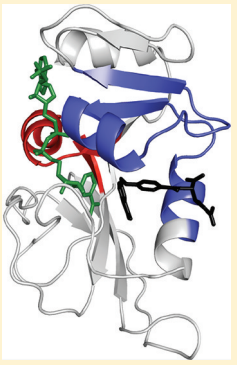

The role of protein motions in enzymatic catalysis is a research area of great interest where much remains to be understood (e.g., refs 1–4). Examining the similarities and differences in the dynamical features of enzyme homologues that catalyze the same reaction affords the opportunity to study the interplay of structure, flexibility, and function.[4,5] Dihydrofolate reductase (5,6,7,8-tetrahydrofolate: $NADP^+$ oxidoreductase, EC 1.5.1.3; DHFR) is a ubiquitous enzyme found in prokaryotes and eukaryotes. It catalyzes the stereospecific transfer of a hydride ion from nicotinamide adenine dinucleotide phosphate (NADPH) cofactor to 7,8-dihydrofolate (DHF) to yield 5,6,7,8-tetrahydrofolate (THF) and oxidized nicotinamide adenine dinucleotide phosphate ($NADP^+$) and is the only source of THF, a one-carbon donor/acceptor unit vital to the biosynthesis of purines, pyrimidines, and amino acids.[6]

X-ray crystallographic studies of mesophilic and thermophilic orthologs, including DHFR enzymes from *E. coli* (*Ec*-DHFR) or *B. stearothermophilus* (*Bs*-DHFR), most commonly reveal nearly identical structures.[7−11] By contrast, the catalytic behaviors of these enzymes diverge. In the case of *Ec*-DHFR, kinetic studies of the hydride transfer step as a function of temperature yielded an enthalpy of activation between 3 and 6 kcal/mol and an isotope effect on the Arrhenius prefactor (A_H/A_D) of 4.0 ± 1.5,[12] compared to an enthalpy of activation of 5.5 ± 0.1 kcal/mol and an isotope effect on A_H/A_D that is inverse for Bs-DHFR.[7] Characteristic of pairs of mesophile–thermophile homologues at room temperature,[13] the rate of hydride transfer for the *E. coli* enzyme exceeds that of *Bs*-DHFR by ca. 10-fold at pH 9.[7] The high nonclassical value for A_H/A_D with *Ec*-DHFR[12] implicates an efficient active site configuration for hydrogen tunneling from the donor (NADPH) to acceptor (DHF) site,[3,13,14] whereas the value of A_H/A_D for *Bs*-DHFR is closer to that seen with low activity mutants of *Ec*-DHFR.[15] The latter has been attributed to the inability of the mutated enzymes to achieve the same degree of active site compression as occurs in the wild-type (WT) enzyme.[14] Such a compromised active site must then undergo local donor–acceptor distance sampling, in order to restore the heavy atom

Received: April 26, 2011
Revised: August 2, 2011
Published: August 22, 2011

ACS Publications © 2011 American Chemical Society

distance that can support tunneling, and is the source of the inverse values for A_H/A_D.[3,13,14]

Hydrogen/deuterium exchange (HDX) offers an excellent probe of the impact of perturbations to protein structure and flexibility by extrinsic parameters, such as pH and temperature (e.g., refs 16−18). The impact of temperature under conditions of EX-2 exchange was recently probed using HDX linked to mass spectrometry (HDX-MS) for *Bs*-DHFR.[18] At the lowest temperature (10 °C) and longest time (300 min), ca. 60% of exchangeable amides in *Bs*-DHFR became deuterated. Most of the peptides derived from *Bs*-DHFR showed relatively small increases in deuteration with increasing temperature, while peptides derived from regions that bridge the cofactor and substrate-binding sites showed a much higher sensitivity to temperature changes. These spatially resolved differences were interpreted in the context of positional differences in apparent ΔH° for local protein unfolding.

Comparison of a number of thermophilic proteins with their mesophilic counterparts at low temperatures indicates increased rigidity in the thermophilic forms, which may occur globally or be localized to specific regions [cf. the studies of indoleglycerol phosphate synthase,[19] xylose isomerase,[20] and *p*-nitrobenzyl esterase[21−24]]. It has been suggested that thermophilic enzymes gain thermostability by reducing conformational flexibility and, as a consequence, sacrifice catalytic efficiency at reduced temperature.[3,22,25] Thus, the increased flexibility of thermophilic proteins at higher temperature mimics the flexibility of mesophilic active sites at their lower physiologically relevant temperature, and this comparative flexibility is associated with optimal protein function.

In the present work, we examine the interplay between protein flexibility and function by comparing the extent of native state deuteration for *Ec*-DHFR close to its functional temperature (25 °C) to the thermophilic variant *Bs*-DHFR at the same temperature, i.e., far below its optimal growth temperature. Spatial resolution is achieved by examining proteolytically generated peptides by HDX-MS. Surprisingly, only a single region within *Ec*-DHFR, which encompasses the interface between bound cofactor and substrate, is more flexible at 25 °C in comparison to *Bs*-DHFR. The remainder of the *Ec*-DHFR shows either the same or reduced flexibility than *Bs*-DHFR at 25 °C. The core peptide of *Ec*-DHFR that is shown to have enhanced flexibility is homologous to the region of *Bs*-DHFR previously demonstrated to undergo regional unfolding with a ΔH°_{unf} value that is similar to the $\Delta H^\ddagger$ for hydride transfer.[7,18] These new data provide further support for models in which the primary enthalpic barrier controlling enzymatic hydrogen tunneling may derive from local, active site fluctuations (protein reorganization).

EXPERIMENTAL PROCEDURES

Protein Purification and Enzyme Assays. NADPH was purchased from Sigma and used without further purification. Dihydrofolate (DHF) was prepared as specified by Blakely et al. and previously described.[26] *Bs*-DHFR was cloned, expressed, purified, and assayed as described,[26] with minor modifications. The final *Bs*-DHFR sample was adjusted to 5.9 mg/mL with a standard buffer (25 mM $KHPO_4$ pH 7.4, 125 mM KCl, and 2.5 mM DTT) and stored in 50 μL aliquots at −80 °C. The *Ec*-DHFR protein, prepared according to established procedures,[12] was exchanged into standard buffer using an Amicon concentrator, followed by a PD10 column (Amersham 17-0851-01) and adjusted to 6.0 mg/mL. The *Ec*-DHFR protein showed k_{cat} = 8.3 s^{-1} in MTEN buffer (pH 7) in the presence of 100 μM DHF and 100 μM NADPH, a rate comparable to previously determined values.

Hydrogen−Deuterium Exchange Mass Spectrometry (HDX-MS) Measurements. Protocols for HDX-MS on pepsin-generated peptides were described in Sours et al.[27] Solutions of Ec-DHFR were incubated at 25 °C in 90% (v/v) D_2O between 0 and 5 h at the same time and under conditions identical to those for *Bs*-DHFR.[18] Approximately 26 min elapsed between the initial acidification and elution of the last peptide from the column. HDX-MS and MS/MS measurements were performed using a Q-Star Pulsar mass spectrometer (Applied Biosystems). Peptides identified and confirmed by MS/MS for *Ec*-DHFR and *Bs*-DHFR[18] are listed in Table S1.

We define the fractional deuteration at time, *t*, as N_t/N_∞, where N_t equals the number of deuterons exchanged into each peptide and N_∞ equals the total number of exchangeable amides (i.e., total peptides bonds minus the number N-terminal to prolines) that should be deuterated at infinite time. The N_t is the difference between the corrected weighted average mass at time *t* (min), $M_{t,corr,BE}$, and *t* = 0 min ($M_{0,corr\ BE}$). Corrections for artifactual in-exchange and back-exchange were calculated as described.[28,29] Calculations of the final D_{300} values (see text) with either average back exchange values, or after correction for faster exchange at the first amide of each peptide, do not alter the conclusions. Time courses of deuteration or fractional deuteration were fit to a two-exponential equation:

$$Y = N_\infty - Ae^{-k_1 t} - Be^{-k_2 t} - \mathrm{NE} \quad (1)$$

where *Y* equals the number of deuterons observed at time = *t*, N_∞ equals the total exchangeable amides, *A* equals the number of amide hydrogens in each peptide exchanging with fast kinetic rate constant, k_1, *B* equals the number of amide hydrogens with slow rate constant, k_2, and NE is the number of amide hydrogens that remain nonexchanging at the longest time point (300 min; $k_{(exchange)} < 0.002\ min^{-1}$).

Controls for the Evaluation of Deuterium Exchange Differences between Ec- and Bs-DHFR. Given the relatively low overall sequence identity between *Ec*-DHFR and *Bs*-DHFR, some portion of the observed deuterium exchange rate differences between these proteins might arise from nearest-neighbor effects on the exchange properties at each position along the protein chain. The intrinsic exchange rate constant (i.e., the HDX of unprotected amide in solution) for each positional amino acid was therefore estimated using the HX2 spreadsheet calculator. This spreadsheet employs user-specified inputs of pH and temperature to calculate the intrinsic exchange rate constant for each amide, depending on side chain identity and position within the polypeptide chain.[30] The values for $k_{int(i)}$ were summed at each position and normalized to the total number of exchanging amides to obtain the average value for each peptide analyzed:

$$k_{int(i)} = \sum_i k_{int(i)}/N_\infty \quad (2)$$

Possible structural origins of the HDX results were also assessed by examining the distance from each amide hydrogen to the protein surface, based on PDB files for *Ec*-DHFR [PDBID: 5DFR (apo) and 1RX2 (with bound NAD^+ and folate) and Bs-DHFR [PDBID: 1ZDR (apo)]. These were estimated from calculations of solvent accessible surface using the program EDTSurf,[31] which was modified to allow exclusion

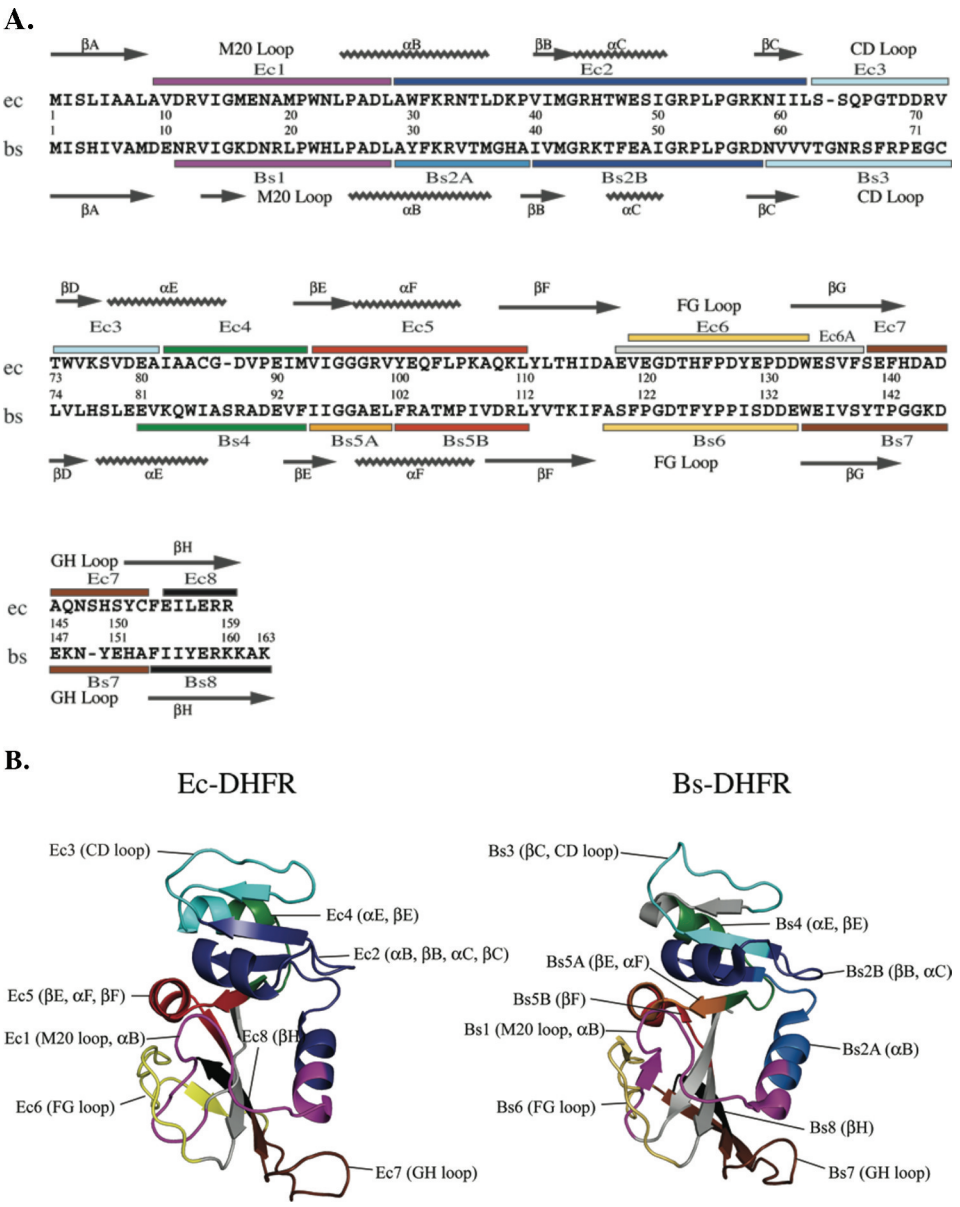

Figure 1. Observed peptides in *Ec*-DHFR and *Bs*-DHFR. (A) Eight nonoverlapping peptides in *Ec*-DHFR and ten nonoverlapping peptides in *Bs*-DHFR, generated by pepsin proteolysis were identified by MS/MS and highlighted against the sequences of the two enzymes. (B) Left panel: observed peptides from *Ec*-DHFR are mapped onto the X-ray structure of the apo-*Ec*-DHFR (PDBID: 5DFR). Right panel: peptides from *Bs*-DHFR are mapped onto the X-ray structure of apo-*Bs*-DHFR (PDBID: 1ZDR). Colors for each peptide correspond to those in panel A.

of internal cavities [Xu, D., personal communication]. In-house scripts were used to calculate distance to surface and are summarized in Table S3. Distances that differed by more than 0.5 Å between *Ec*-DHFR and *Bs*-DHFR were scored as significant changes. Additionally, the pattern of H-bonding interactions was estimated, in which the amide nitrogen acts as an H-donor and any oxygen or nitrogen atom can serve as hydrogen acceptor. All possible H-donor/acceptor distances up to 3.5 Å were filtered by a further constraint requiring hydrogen bond angle >120°.

RESULTS

The eight nonoverlapping *Ec*-DHFR peptides identified by LC-MS/MS and selected for HDX-MS analysis (Table S1) covered 138 of 159 (87%) amino acids in the *Ec*-DHFR primary sequence. The same peptides were detected by Yamamoto et al.[32] in a prior hydrogen exchange analysis of *Ec*-DHFR performed at 15 °C, indicating reproducibility of pepsin digestion. Ten nonoverlapping peptides previously reported for *Bs*-DHFR which covered 142 of 164 (87%) amino acids[18] are included in Table S1 for comparison to peptides from *Ec*-DHFR. Figure 1A shows peptides of *Ec*-DHFR aligned against those obtained from *Bs*-DHFR. Peptides from *Ec*-DHFR are longer (average 19 amino acids) than those from *Bs*-DHFR (average 13 amino acids), indicating differences in protease cleavage between these orthologs. Observed peptides are highlighted on the X-ray structures of apo *Ec*-DHFR (PDBID: 5DFR[10]) and apo-*Bs*-DHFR (PDB1D: 1ZDR[7]) (Figure 1B) and labeled next to corresponding α-helix, β-sheet, or loop secondary structures. For both enzymes, HDX-MS was performed in the absence of cofactor or substrate. This condition allowed for the observation of greater HDX, i.e., without the complication of cofactor/substrate protection; the

dx.doi.org/10.1021/bi200640s | *Biochemistry* 2011, 50, 8251–8260

Table 1. Summary of HDX into Peptides from *Ec*-DHFR and *Bs*-DHFR

peptide	residues	structural element	N_∞ [a]	$N_{300\ min}$ [b]	$D_{300\ min}$ [c]	sum k_{int} (min^{-1})	avg k_{int} (min^{-1})
*Ec*1	9−28	M20 loop	17	13.4	0.79	6277	348
*Bs*1	11−28		15	11.1	0.74	7263	453
*Ec*2	29−62	αB, βB, αC, βC	30	22.1	0.74	17372	560
*Bs*2A, 2B	29−58		26	24.4	0.94	13686	488
*Ec*3	63−81	CD loop	17	12.6	0.74	8248	458
*Bs*3	59−73		13	11.8	0.91	11568	826
*Ec*4	82−92	αE	9	5.6	0.62	5940	594
*Bs*4	81−94		13	11.4	0.88	4804	343
*Ec*5	93−110	αF, βF	16	14.1	0.88	6914	406
*Bs*5A, 5B	95−112		15	8.9	0.59	5781	340
*Ec*6	119−133	FG loop	12	6.0	0.50	5484	322
*Bs*6	119−134		12	8.3	0.69	5325	409
*Bs*6	119−134		12	8.3	0.69	5325	409
*Ec*7	138−152	GH loop	14	8.5	0.61	15957	1063
*Bs*7	135−154		17	11.6	0.68	9687	538
*Ec*8	154−159	βH	5	4.5	0.90	6850	1141
*Bs*8	155−164		9	4.7	0.52	2692	269

[a]Number of exchangeable amides, calculated as the number of peptide bonds minus those N-terminal to proline. [b]Observed deuteration at 300 min, 25 °C. [c]Fractional in-exchange at 300 min, 25 °C, $D_{300\ min} = N_{300\ min}/N_\infty$.

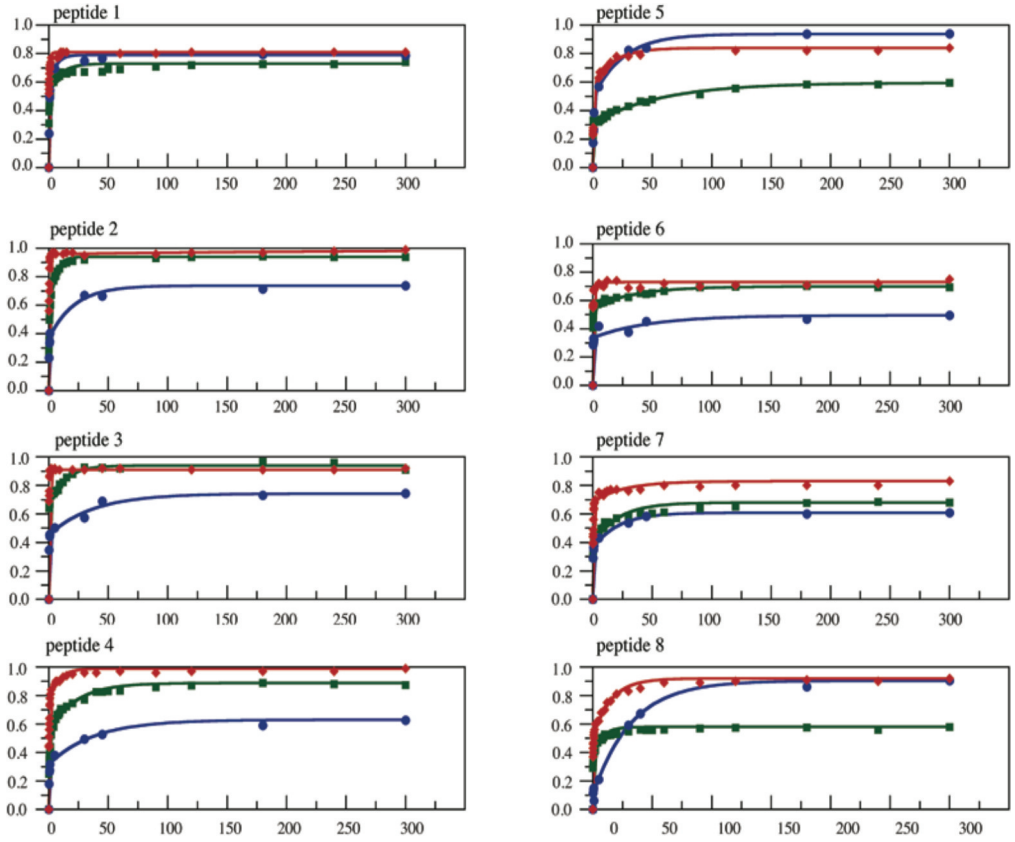

Figure 2. Time courses of fractional deuteration for peptides derived from *Ec*-DHFR (blue, 25 °C) and *Bs*-DHFR (green, 25 °C; red, 55 °C). Peptide pairs are (A) *Ec*1, *Bs*1, (B) *Ec*2, *Bs*2A + *Bs*2B, (C) *Ec*3, *Bs*3, (D) Ec4, *Bs*4, (E) *Ec*5, *Bs*5A + *Bs*5B, (F) *Ec*6, *Bs*6, (G) *Ec*7, *Bs*7, and (H) *Ec*8, *Bs*8. *X*-axis indicates time of incubation in D_2O; *Y*-axis indicates the extent of deuteration at each time point, divided by the number of exchangeable amides in each peptide.

latter was expected to impair our ability to compare core regions of *Ec*-DHFR to *Bs*-DHFR. Studies of other proteins have revealed that while substrates can shift the equilibrium distribution of conformational substates, they do not necessarily generate new substates.[2] In the case of carboxypeptidase B, no detectable difference in HDX-MS was observed in the absence or presence of substrate.[33]

HDX-MS measurements showed similar net deuteration into *Ec*-DHFR and *Bs*-DHFR under matching experimental conditions. This can be seen after 300 min, where the fractional

dx.doi.org/10.1021/bi200640s | *Biochemistry* 2011, 50, 8251−8260

hydrogen exchange summed over all analyzed peptides from each enzyme reached 72% in *Ec*-DHFR and 74% in *Bs*-DHFR (Table 1).[a] Since the peptides listed in Table 1 account for 87% of the full-length sequences for *Bs*- and *Ec*- DHFR, the data in Table 1 are a good approximation of overall deuteration. Thus, although greater overall rigidity might be expected for a thermophilic enzyme, which shows ca. 10-fold less rapid hydride transfer than its mesophilic ortholog at 25 °C, the global exchange rates were comparable.

We then examined variations in HDX by comparing peptides paired between each enzyme. Because the specific pepsin cleavage positions were different, resulting in nonequivalent peptides that could not be exactly aligned, we used two methods to enable comparison of the mesophilic and thermophilic enzymes. First, when possible, shorter peptides from one enzyme were "bundled" together in order to match a longer peptide from the other enzyme. This was feasible for peptides *Bs*2A + *Bs*2B and peptides *Bs*5A + *Bs*5B from thermophilic DHFR, which could respectively be aligned against *Ec*2 and *Ec*5 in the mesophilic enzyme. Second, we report the extent of deuteration normalized by the number of exchangeable amides in each peptide in order to adjust for the differences in peptide length and/or sequence between the two DHFRs.

Time courses for incorporation of deuterium into individual peptides are shown in Figure 2, matching the peptides in *Ec*-DHFR to those with overlapping sequences in *Bs*-DHFR. Estimates of parameters describing the numbers of amides exchanging with fast and slow rate constants were calculated by nonlinear least-squares fitting and are summarized in Table S2. As in our analysis of HDX-MS in the *Bs*-DHFR,[18] the observed rates of exchange in *Ec*-DHFR are very rapid and, overall, less reliable than the extent of exchange at the plateau region reached at long times (ca. 300 min in Figure 2). In Table 1, we report the fractional deuteration (D), calculated as the number of hydrogens observed to have exchanged at 300 min ($A + B$, eq 1) normalized by the number of exchangeable amide hydrogens in each peptide, N_∞.

One factor that may become important in comparing HDX between orthologs is the influence of different peptide sequences on values of the chemical exchange rate constant, k_{int}, in eq 3:

$$k_{obs} = K_{open}k_{int} \quad (3)$$

where k_{obs} is the observed rate of HDX under the current EX-2 condition and K_{open} is the equilibrium constant for the transient local opening of protein to a state that allows chemical exchange. The earlier studies on *Bs*-DHFR at pH 7 showed mass spectrometric patterns in support of an exchange mechanism in which protein undergoes local rapid opening and closing (EX-2), followed by a slow, rate-determining chemical exchange from the peptide amides.[18] Because the amide chemical exchange varies with each amino acid side chain, as well as the amino acid both N-terminal and C-terminal to the amide hydrogen,[30] a divergence of sequences for peptides derived from orthologous proteins could limit direct comparison of rate constants. As summarized in Table 1, variations in average intrinsic rate constants ($k_{int(av)}$) for peptides aligned between *Ec*-DHFR and *Bs*-DHFR went from a high of 87% to a low of 24% among the eight peptide pairs; importantly, there is no consistent covariation between changes in $D_{300\,min}$ and the average k_{int}. As will be discussed below, two peptides (3 and 8) with a large variation in k_{int} that tracked a significant change in $D_{300\,min}$ have been eliminated from consideration for a variety of reasons.

Examination of individual peptides showed important regional variations in HDX behavior between the two enzymes. Two regions showed greater hydrogen exchange into *Ec*-DHFR compared to *Bs*-DHFR, peptides 5 and 8. Because of the poor alignment between the *Ec*8 and *Bs*8 peptides, the observed differences were not considered mechanistically significant (see discussion below). However, peptide *Ec*5 aligns exactly with peptides *Bs*5A and *Bs*5B, encompassing helix αF and part of βF, which comprise the nicotinamide-binding site of each enzyme (Figure 1B). *Ec*5 has 16 exchangeable amides, of which 14.1 (88%) exchanged at 300 min, whereas *Bs*5A and *Bs*5B together have 15 exchangeable amides, of which 8.9 (59%) exchanged (Figure 2 and Table 1). Thus, the extent of deuteration in *Ec*5 was at least 4 Da greater than *Bs*5A + *Bs*5B, which could not be accounted for by the difference in number of exchangeable sites. In *Bs*-DHFR, αF-βF was among the areas most highly protected from hydrogen exchange, reaching 59% at 25 °C (Table 1), but dramatically increasing to 97% as the temperature was raised to 55 °C.[18] Thus, this region showed one of the highest apparent enthalpic changes of local unfolding in *Bs*-DHFR, which has been proposed to control the efficiency of nuclear tunneling during hydride transfer.[18]

Intriguingly, two regions showed lower hydrogen exchange into *Ec*-DHFR compared to *Bs*-DHFR. Paired with *Ec*2 are peptides *Bs*2A and *Bs*2B, which together contain 30 amino acids aligned starting at the N-terminus of *Ec*2 (Figures 1A and 2). Whereas 22.1 of the 30 (74%) exchangeable amides in *Ec*2 were deuterated by 300 min, 24.4 of the 26 (94%) exchangeable amides in *Bs*2A + *Bs*2B were deuterated (Table 1), indicating that at least two amides within this domain underwent exchange in *Bs*-DHFR but were nonexchanging in *Ec*-DHFR. Likewise, peptide *Ec*4 and *Bs*4, corresponding to helix αE and strand βE, were each aligned at their C-terminus (Figures 1A and 2). In *Ec*4 and *Bs*4, 5.6 of the 9 exchangeable amides (62%) and 11.4 of the 13 exchangeable amides (88%), respectively, underwent deuteration (Table 1). Although *Bs*4 contains four more exchangeable amides than *Ec*4, its deuteration exceeded that of *Ec*4 by 6 Da, revealing that two amides which were nonexchanging in *Ec*4 were allowed to exchange in *Bs*4. Peptides *Ec*2 and *Bs*2 contain helices αB and αC and strands βB and βC, while peptides *Ec*4 and *Bs*4 contain helix αE and strand βE. Together, these regions comprise most of the adenosine-binding subdomain, revealing high conformational mobility in *Bs*-DHFR that is suppressed in *Ec*-DHFR.

The remaining areas showed few differences between mesophilic and thermophilic DHFR. Peptides *Ec*1 and *Bs*1 encompass the M20 loop and helix αB in each enzyme (Figure 1B). *Ec*1 has 17 exchangeable amides, of which 13.4 (79%) exchanged at 300 min, whereas *Bs*1 has 15 exchangeable amides, of which 11.1 (74%) exchanged (Table 1). The additional two deuteration events in *Ec*1 could be accounted for by the longer length of this peptide compared to *Bs*1; thus, the degree of exchange might be similar between *Ec*- and *Bs*-DHFR within the region of overlap.

Peptides *Ec*3 and *Bs*3 include the CD loop. *Bs*3 contains 13 exchangeable amides, of which at 12 (91%) exchanged after 300 min, whereas *Ec*3 contains 17 exchangeable amides, of which 13 (74%) exchanged. Each peptide is offset from the other by several residues, whereby *Bs*3 adds 4 residues N-terminal to the start of *Ec*3, and *Ec*3 adds 9 residues past the C-terminus of *Bs*3 (Figure 1A). The area directly aligned between these peptides

covers only 8 and 9 exchangeable amides in *Ec*3 and *Bs*3, respectively. Most of these residues would be expected to exchange in *Bs*, and a comparable level of exchange within this region in *Ec*3 could not be excluded. Thus, the comparison does not necessarily reveal differences in deuteration in *Ec*3 compared to *Bs*3. Likewise, *Ec*6 and *Bs*6, covering the FG loop, showed significantly lower HDX into *Ec*-DHFR than *Bs*-DHFR (Figure 1B and Table 1). This could, in principle, reflect enhanced conformational mobility or solvent accessibility within *Bs*-DHFR compared to *Ec*-DHFR. However, because *Bs*6 included two additional amides N-terminal to the start of the *Ec*6 sequence, the possibility that their corresponding hydrogens exchanged by 300 min and accounted for the increased HDX in *Bs*6 could not be excluded. Indeed, the amide hydrogens corresponding to Ser120 and Phe121 were highly solvent exposed in the X-ray structure of *Bs*-DHFR (1ZDR) (data not shown), consistent with an expectation of their rapid exchange. A similar argument could be made for *Ec*7 and *Bs*7, which included 14 and 17 exchangeable amides, respectively. Although *Bs*7 was deuterated more than *Ec*7 by ~3 Da, the additional deuteration could not be ascribed unambiguously to the region of overlap (Table 1). Finally, the C-terminal peptides, *Ec*8 and *Bs*8, differ in length by almost 2-fold. Nonetheless, they both exchanged between 4 and 5 hydrogens at 300 min, which may well have arisen from a region in *Bs*8 which overlaps completely with *Ec*8.

The results above suggested that *Bs*-DHFR and *Ec*-DHFR differ in conformational mobility within several regions, represented by peptides 2, 4, and 5. However, because the two enzymes share only partial sequence identity, it was important to be certain that differences in solution hydrogen exchange were not due to differences in structure between the two enzymes. Therefore, X-ray coordinates of apo-enzymes *Bs*-DHFR (1ZDR) and *Ec*-DHFR (5DFR) were compared, in each case examining the aligned structures for differences in solvent accessibility of amide hydrogens that might be the cause of observed differences in deuteration. This analysis focused on the peptide pairs *Ec*2-*Bs*2A/2B, *Ec*4-*Bs*4, and *Ec*5-*Bs*5.

Peptides *Ec*5, *Bs*5A, and *Bs*5B cover the only region which displayed higher HDX in *Ec*-DHFR than *Bs*-DHFR. Tertiary structures, distances of amide hydrogens to surface, and hydrogen bond lengths and angles were compared in this region to assess structural changes which might account for the ≥5 Da difference in deuteration. In general, residues and amide hydrogens superimposed well (Figure 3A), although at least four amide hydrogens showed a shorter distance to surface in *Bs*-DHFR than *Ec*-DHFR, primarily due to reduced steric interactions with side chains and/or backbone angles which tilted these atoms toward solvent (Table S3); one amide hydrogen showed longer distance to surface in *Bs*-DHFR than *Ec*-DHFR. With regard to hydrogen bonds satisfying the condition <3.5 Å and >120°, two amides were identified in *Bs*5A and *Bs*5B that had no corresponding interactions in *Ec*5 (Table S3). Overall, the tertiary structures indicated greater protection of amide hydrogens from solvent in *Ec*-DHFR, contrary to the HDX behavior. This supports the conclusion that the increased deuteration of *Ec*5 compared to *Bs*5A + *Bs*5B reflects enhanced conformational mobility in the mesophilic over the thermophilic enzyme in this region.

Peptides *Ec*2/*Bs*2A + *Bs*2B and *Ec*4/*Bs*4 showed significantly higher deuteration into *Bs*-DHFR than *Ec*-DHFR. In *Ec*2 and *Bs*2A + *Bs*2B, the backbone structures and amide hydrogen positions overlapped well (Figure 3B). Distance to surface

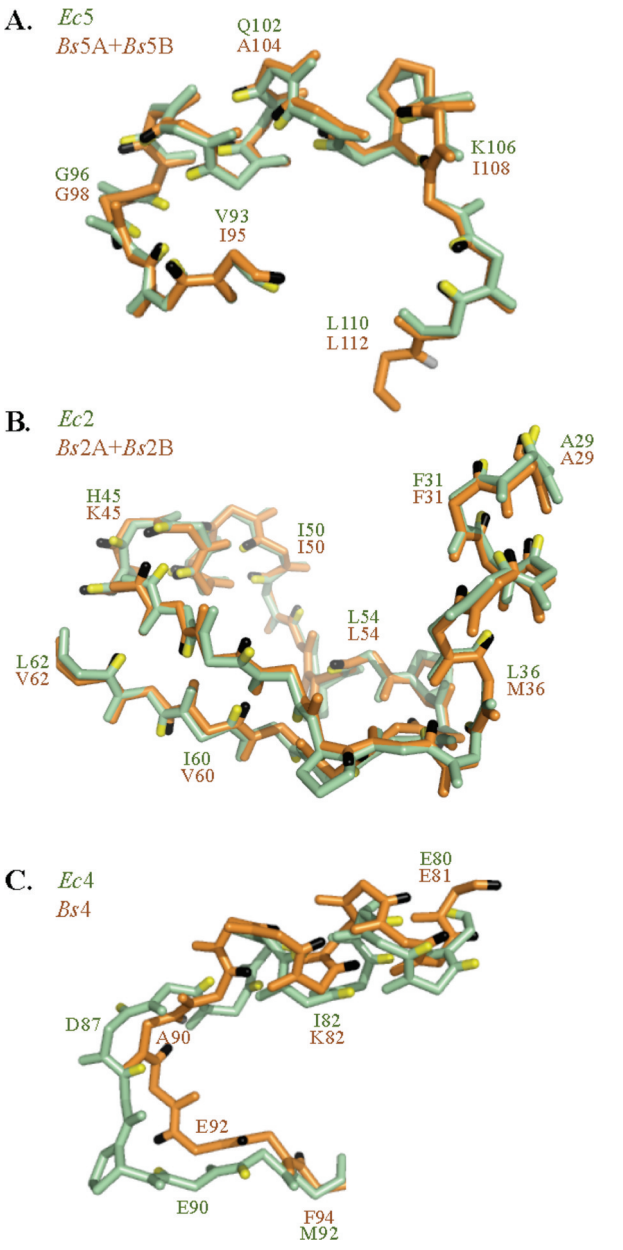

Figure 3. Structural comparison of peptides from *Ec*-DHFR and *Bs*-DHFR. Peptide pairs are (A) *Ec*5 and *Bs*5A + *Bs*5B, (B) *Ec*2 and *Bs*2A + *Bs*2B, and (C) *Ec*4 and *Bs*4, showing peptides from *Ec*-DHFR in green and peptides from *Bs*-DHFR in brown. Backbone amide hydrogens in peptides *Ec*5 and *Bs*5A + *Bs*5B as well as peptides *Ec*2 and *Bs*2A + *Bs*2B overlay well, suggesting that differences in HDX in these regions reflect changes in conformational mobility. Backbone amide hydrogens in peptides *Ec*4 and *Bs*4 show structural deviations which suggest greater protection of *Bs*-DHFR from solvent, opposite to the effects on HDX. The amide hydrogens in *Ec*- and *Bs*-DHFR are indicated in yellow and black, respectively.

measurements suggested higher protection from solvent in *Bs*-DHFR than *Ec*-DHFR for six amide hydrogens and smaller protection for four amide hydrogens, mostly due to differences in side chain orientation. We observed no examples where hydrogen-bonding patterns were disrupted in one enzyme but not the other. Thus, we observed no clear-cut differences in structure around *Ec*2 and *Bs*2A/*Bs*2B, for which we might expect higher HDX in the thermophilic enzyme.

On the other hand, *Ec*4 and *Bs*4, occurring in the surface loop between helix αE and βE, showed significant deviations in structure, from their N-termini up to where residues Pro89 in *Ec*-DHFR and Asp91 in *Bs*-DHFR again superimposed (Figure 3C). Here, the *Bs*4 backbone formed a loop that was constrained by cation−pi interactions between Trp85 and Arg89 side chains, whereas the *Ec*4 backbone showed less restriction. Thus, direct comparisons could not be made between the two enzymes in this region. Nevertheless, distance to surface calculations showed that all five amides corresponding to residues 85−89 in *Bs*-DHFR were buried by 0.8−2.4 Å from the surface, whereas only three amides for the corresponding residues 83−87 in *Ec*-DHFR were buried (0.5−1.9 Å), while two amides were fully exposed to solvent (Table S3). Because of this, hydrogen bonds at two amides in *Bs*4 were absent at the same positions in *Ec*4. Thus, on the basis of structure, *Bs*4 might be expected to show more protection from exchange than *Ec*4, in contrast to the observed HDX behavior. The results indicate that the increased deuteration in *Bs*-DHFR in these two regions is unlikely to arise from structural differences and, instead, reflects enhanced conformational mobility in the thermophilic enzyme over the mesophilic enzyme.

DISCUSSION

Spatially Resolved HDX as a Probe of Temperature Adaptation in Protein Flexibility for a Thermophilic vs Mesophilic Variant of DHFR. A robust approach to understanding the relationship of protein motions to enzyme catalysis is to examine orthologous proteins that have evolved to function in different temperature niches. The availability of structurally similar DHFRs from a thermophilic (*Bs*-DHFR) and mesophilic (*Ec*-DHFR) source (cf. Figure 1B) has been exploited in the present work. The "corresponding state hypothesis"[25] predicts that a protein that functions normally at elevated temperature will become more rigid at reduced temperatures, reflecting the presence of interactions that allow for protein stability at the elevated, physiologically relevant temperature. At the same time, the elevation of temperature enables the thermophilic protein to become flexible in regions of the protein that control either the binding and release of substrates/products or the bond cleavage events. In this manner, thermophilic proteins can solve the combined need of stability and function at elevated temperatures.

The dihydrofolate reductase from *E. coli* (*Ec*-DHFR) is a much studied mesophilic protein from the perspective of both protein dynamics and chemical catalysis. X-ray studies have demonstrated that a flexible (M20) loop can assume different conformations (open, closed, and occluded), and NMR studies showed that these conformational changes occur on the same time scale as the progression of enzyme from substrate to product complexes.[34] In a recent study of a thermophilic variant of DHFR (*Bs*-DHFR) by HDX-MS, a method was introduced for evaluating enthalpic changes that correspond to local protein unfolding events and their comparison to the enthalpic barrier of catalysis. A relevant finding was that the motions corresponding to the enthalpic barrier for hydride transfer were restricted to the central core of the protein near the region of contact between cofactor and substrate.[18]

In the present work, we have extended our study of HDX-MS to the *Ec*-DHFR in an effort to examine similarities and differences between the two proteins under the 25 °C condition that *Ec*-DHFR functions. In particular, we wanted to determine whether the expected enhanced mobility for the *Ec*-DHFR at 25 °C would occur throughout the entire protein or be restricted to specific regions of protein such as the one that intersects the $NADP^+$ and substrate-binding pockets and the surface loops. The net deuterium exchange at long times into both proteins is quite similar, reinforcing the necessity to analyze and compare individual peptides in order to detect possible differences in local flexibility. Following the use of pepsin to digest the *Ec*-DHFR into small peptides for analysis of time-dependent deuterium exchange, a total of eight unique peptides were chosen (87% coverage of the total protein), for comparison to peptides chosen from the previous analysis of *Bs*-DHFR[18] (87% coverage) (Figure 1).

Although the tertiary structures for *Ec*- and *Bs*-DHFR are almost identical[7] (Figure 1B), significant differences exist in their primary sequences. As a consequence, the position of cleavage into peptides after exposure to the protease pepsin was different for the DHFR variants, leading to nonequivalent peptides for comparison. We were able to overcome this barrier, in part, by using the technique of bundling shorter peptides obtained from *Bs*-DHFR to match longer peptides in *Ec*-DHFR (in the case of peptides 2 and 5). A second factor that will influence a comparison of rates of deuterium incorporation into the backbone amides of orthologous proteins with divergent primary sequences is the intrinsic rate constant for chemical exchange (k_{int}, eq 3). Thus, a calculation of composite, average intrinsic exchange rate was carried out for each peptide (Experimental Procedures). As summarized in Table 1, this type of comparative analysis for *Ec*- and *Bs*-DHFR showed no consistent covariation in k_{int}(avg) and $D_{300\ min}$, with the majority of peptides yielding similar values for k_{int}(avg). This property, together with the previously noted large errors in the rate constants for fast (k_1) and intermediate (k_2) exchange rate constants in *Bs*-DHFR,[18] led us to focus on the plateau regions of the time courses, which reflect the very slow, effectively nonexchanging, amide hydrogens ($k_3 < 0.002\ min^{-1}$) on the time scale of the experiments (300 min).

From the summary of such plateau data for *Ec*-DHFR and *Bs*-DHFR at 25 °C (Table 1) and accompanying analyses, it can be seen that three peptides show a clear distinction: peptide 5, which indicates more complete exchange in *Ec*-DHFR, and peptides 2 and 4, which indicate less exchange into the mesophilic protein. That these differences reflect local differences in protein flexibility is supported and reinforced by a structural analysis of the distance from each peptide hydrogen to the solvent surface (Figure 3 and Table S3) in the intact protein structures. Thus, while the average deuterium exchange into intact *Ec*- and *Bs*-DHFR is almost identical at 25 °C, significant differences in flexibility between the two proteins emerge when spatial resolution is introduced via the proteolytic digestion of protein to allow peptide analysis by mass spectrometry.

Relevance of Observed Patterns for HDX in Ec-DHFR and Bs-DHFR to Protein Motions Affecting the Hydride Transfer Step. Although certain regions of the *Ec*- and *Bs*-DHFR were not available for direct comparison, it is fortunate that peptides representing functionally important regions of the protein could be contrasted. These include (1) the M20 and FG loops, which change their position during the catalytic cycle in WT Ec-DHFR,[34] (2) the binding domains that surround the adenosine ring of the NADPH cofactor and the polyglutamate tail of the DHF substrate, and (3) a region of protein which

includes active site residues near the reactive portions of NADPH and DHF.

In a recently published work, a method for extracting apparent enthalpies for local protein unfolding, ΔH°_{unf}, was introduced. Among the 11 *Bs*-DHFR peptides studied, all but two showed very small values for ΔH°_{unf} that were ≤2 kcal/mol. These included peptides 1, 2−4, and 6−8 (using the numbering system of the present study). It was proposed[18] that each of these low-enthalpy regions of protein would contribute dominantly to the conformational sampling (preorganization) which generates hydrogen tunneling-ready geometries (peptides 2−4, 7, and 8) and/or to the changes in protein structure which accompany the progression of the ES complex through the catalytic cycle (peptides 1 and 6).[34] As discussed in detail in several recent reviews,[3,14] two classes of protein motions appear essential for enzyme-catalyzed H-tunneling, termed preorganization and reorganization (see below). The preorganization process represents a sampling of protein conformational substates, with only a subset of these being capable of achieving the hydrogen tunneling-appropriate geometries. A low enthalpic barrier between conformational substates may be desired from an evolutionary perspective, ensuring a smooth conformational landscape that prevents the trapping of protein into nonproductive conformers.

It is of considerable interest that the majority of the comparable peptides in the *Ec*-DHFR show little discernible difference in relation to *Bs*-DHFR. It appears that for regions of a thermophilic protein that display high flexibility at the elevated, functional temperature, the additional property of small enthalpic barriers for local unfolding may be predictive of positions with comparable flexibility within a mesophilic ortholog at its reduced, functional temperature. Among the peptides with comparable extent of exchange in *Ec*- as *Bs*-DHFR are those representing the M20 and FG loops.

A second important insight from the earlier study of *Bs*-DHFR was the identification of two regions of protein with a pronounced temperature dependence for local protein unfolding: peptide 1, which was not available for comparison between the *Ec*- and *Bs*-DHFRs, and peptide 5, characterized in the present study. *It is most significant that, among the peptides from Ec-DHFR that could be quantitatively compared to Bs-DHFR, peptide 5 is the only one that indicates enhanced flexibility within the Ec-DHFR at* 25 °C (Figure 4). It is further notable that the E_a of 3−6 kcal/mol for the hydride transfer catalyzed by *Ec*-DHFR[12] is comparable to the apparent enthalpy of unfolding measured for the region corresponding to region 5 in *Bs*-DHFR, ΔH°_{unf} = 3.8 kcal/mol.[18] While this result could simply be fortuitous, the combination of our earlier study of *Bs*-DHFR[18] and the present study point toward a key structural element that resides within the active site of DHFR and controls a large portion of the enthalpic barrier for H-tunneling. We had previously proposed that the enthalpic barrier for hydride transfer in *Bs*-DHFR was likely to be dominated by local structural rearrangements (reorganization) that influence the hydrogenic donor−acceptor wave function overlap and not from loop motions that would include the closed to occluded transition in the M20 loop.[18] In a very recent study that combines NMR dispersion data with X-ray crystallography, Wright and co-workers suggest that hydride transfer in *Ec*-DHFR is linked to millisecond motion within the protein core rather than the M20 loop.[35] Reorganization arises from the need for changes in the electrostatic environment in order to transiently generate energetic degeneracy between reactant and product, together with any necessary adjustments in the donor/acceptor distance *R*.[4,14]

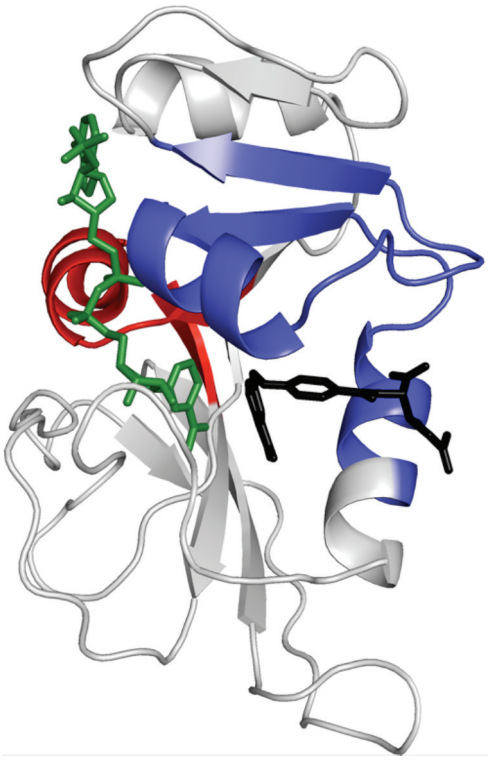

Figure 4. Variations in HDX between *Ec*-DHFR and *Bs*-DHFR. Colored against the backbone structure of *Ec*-DHFR (1RX2) are areas where HDX in *Ec*-DHFR exceeds *Bs*-DHFR (red), *Bs*-DHFR exceeds *Ec*-DHFR (blue), or little differences are observed between the two enzymes (gray).

The enthalpies of activation for hydride transfer for both *Bs*-DHFR (E_a = 5.5 ± 0.1 kcal/mol) and *Ec*-DHFR (E_a = 3−6 kcal/mol) are small and quite similar. Although there is considerable uncertainty in E_a for *Ec*-DHFR, an elevated value of E_a for *Bs*-DHFR could be indicative of an enzyme active site that is less optimized for hydrogen tunneling, as suggested from the larger temperature dependence of the KIE (A_H/A_D = 0.57)[7] in relation to *Ec*-DHFR (A_H/A_D = 4.0).[12]

In addition to the above trends, there is the observation of two peptides (2 and 4) in *Ec*-DHFR *which are less flexible than the comparable peptides in Bs-DHFR* (Figure 4). This is not the first instance in which a reduced temperature enzyme shows restricted motion in relation to its corresponding high-temperature ortholog. In a study of homologous, temperature-adapted forms of a prokaryotic alcohol dehydrogenase near their functional temperatures of 65 °C (thermophilic variant) and 5 °C (psychrophilic variant), families of peptides were identified that exchanged either more or less at the reduced temperature of the psychrophile.[36] The regions that showed greater extent of exchange were, for the most part, interior to the protein and abutting regions near the nicotinamide ring of cofactor and the substrate. By contrast, the regions showing less exchange tended to be clustered closer to the periphery of the protein and to form an enclosure surrounding the faster exchanging region.[36] In the case of the *Ec*-DHFR, the observation of a restriction of motions within secondary structural units that interact with the nonreacting ends of the bound cofactor (at its adenosine ring) and substrate (at the polyglutamate tail) is in marked contrast to the behavior

dx.doi.org/10.1021/bi200640s | *Biochemistry* 2011, 50, 8251−8260

of peptide 5 that lies closer to the region of hydride transfer. It is likely that the reduced motions in these remote regions of cofactor and substrate binding play some role in catalysis, although it is difficult to distinguish whether this is related to the binding and positioning of cofactor and substrate or the subsequent rate of hydride transfer.

CONCLUSIONS

The comparison of orthologous DHFRs (the mesophilic *Ec*-DHFR to the thermophilic *Bs*-DHFR) at 25 °C by HDX-MS identifies three distinct classes of differential conformational flexibility. The majority of peptide fragments from both proteins suggest similar native state HDX behavior; additionally, a single peptide shows greater flexibility for *Ec*-DHFR and two peptides show reduced flexibility (Figure 4). The region of greater flexibility in *Ec*-DHFR at 25 °C maps to the region previously identified in *Bs*-DHFR as controlling the enthalpic barrier for H-tunneling from NADPH to DHF in *Bs*-DHFR.[18] This catalysis-linked peptide is derived from the core of the protein rather than any of the flanking loops.

ASSOCIATED CONTENT

Supporting Information

Peptides identified from each protein, kinetic parameters for HDX, the distance to surface calculations for each peptide bond, and the hydrogen bond distances and angles for each peptide bond. This material is available free of charge via the Internet at http://pubs.acs.org.

AUTHOR INFORMATION

Corresponding Author

*E-mail klinman@berkeley.edu, Ph 510-642-2668, Fax 510-643-6232 (J.P.K.). E-mail Natalie.Ahn@Colorado.edu, Ph 303-492-4799, Fax 303-492-2439 (N.G.A.).

Funding

This work was supported by grants to J.P.K. (NIH R01 GM025765, NSF MCB0446395), N.G.A. (NIH R01 GM074134), O.A.O. (NIH T32 GM08295), and A.K. (NSF CHE-0715448, BSF 2007256).

Notes

[⊥]Deceased January 8, 2009.

ACKNOWLEDGMENTS

The authors are indebted to Dr. Dong Xu (U. Michigan) for modifying the EDTSurf program to allow the option of excluding internal cavities, to Adam Ring (Colorado State University) for generating distance to surface and hydrogen bond distance and angle measurements, to Kelli Markham and Todd Fleischmann (U. Iowa) for providing *Ec*-DHFR, to Dr. Steven Damo (Vanderbilt University) for assistance in purifying *Bs*-DHFR, and to Prof. David Wemmer (UC Berkeley) for valuable discussions.

ABBREVIATIONS

DHFR, dihydrofolate reductase; DHF, dihydrofolate; THF, tetrahydrofolate; DTT, dithiothreitol; MES, 2-(*N*-morpholino)-ethanesulfonic acid; HDX, hydrogen−deuterium exchange; HDX-MS, hydrogen−deuterium exchange by mass spectrometry; T_m, melting temperature; KIE, kinetic isotope effect; *Ec*-DHFR, *Escherichia coli* dihydrofolate reductase; *Bs*-DHFR, *Bacillus stearothermophilus* dihydrofolate reductase; SDS-PAGE, sodium dodecyl sulfate polyacrylamide gel electrophoresis; LC-MS, liquid chromatography/mass spectrometry; LC-MS/MS, liquid chromatography and mass spectrometric fragmentation; MTEN buffer, 50 mM 2-(*N*-morpholino)ethanesulfonic acid, 25 mM tris(hydroxymethyl)aminomethane, 25 mM ethanolamine, and 100 mM NaCl.

ADDITIONAL NOTE

[a]We note that an earlier conclusion of lower exchange into *Bs*-DHFR in comparison to *Ec*-DHFR[18] was based on published data for the *E. coli* enzyme at 15 °C. We believe the conclusion in the current study is more accurate because it compares matching experimental conditions for both enzymes.

REFERENCES

(1) Hammes-Schiffer, S., and Benkovic, S. J. (2006) Relating protein motion to catalysis. *Annu. Rev. Biochem. 75*, 519−541.

(2) Henzler-Wildman, K. A., Lei, M., Thai, V., Kerns, S. J., Karplus, M., and Kern, D. (2007) A hierarchy of timescales in protein dynamics is linked to enzyme catalysis. *Nature 450*, 913−916.

(3) Nagel, Z. D., and Klinman, J. P. (2009) A 21st century revisionist's view at a turning point in enzymology. *Nat. Chem. Biol. 5*, 543−550.

(4) Schwartz, S., and Schramm, V. L. (2009) Enzymatic transition states and dynamic motion in barrier crossing. *Nat. Chem. Biol. 5*, 551−558.

(5) Fields, P. A. (2001) Review: Protein function at thermal extremes: balancing stability and flexibility. *Comp. Biochem. Physiol., Part A: Mol. Integr. Physiol. 129*, 417−431.

(6) Liang, Z.-X., Tsigos, I., Bouriotis, V., and Klinman, J. P. (2004) Impact of protein flexibility on hydride-transfer parameters in thermophilic and psychrophilic alcohol dehydrogenases. *J. Am. Chem. Soc. 126*, 9500−9501.

(7) Kim, H. S., Damo, S. M., Lee, S. Y., Wemmer, D., and Klinman, J. P. (2005) Structure and hydride transfer mechanism of a moderate thermophilic dihydrofolate reductase from *Bacillus stearothermophilus* and comparison to its mesophilic and hyperthermophilic homologues. *Biochemistry 44*, 11428−11439.

(8) Bolin, J. T., Filman, D. J., Matthews, D. A., Hamlin, R. C., and Kraut, J. (1982) Crystal structures of *Escherichia coli* and *Lactobacillus casei* dihydrofolate reductase refined at 1.7 Å resolution. I. General features and binding of methotrexate. *J. Biol. Chem. 257*, 13650−13662.

(9) Filman, D. J., Bolin, J. T., Matthews, D. A., and Kraut, J. (1982) Crystal structures of *Escherichia coli* and *Lactobacillus casei* dihydrofolate reductase refined at 1.7 Å resolution. II. Environment of bound NADPH and implications for catalysis. *J. Biol. Chem. 257*, 13663−13672.

(10) Bystroff, C., and Kraut, J. (1991) Crystal structure of unliganded *Escherichia coli* dihydrofolate reductase. Ligand-induced conformational changes and cooperativity in binding. *Biochemistry 30*, 2227−2239.

(11) Bystroff, C., Oatley, S. J., and Kraut, J. (1990) Crystal structures of *Escherichia coli* dihydrofolate reductase: the NADP+ holoenzyme and the folate. NADP+ ternary complex. Substrate binding and a model for the transition state. *Biochemistry 29*, 3263−3277.

(12) Sikorski, R. S., Wang, L., Markham, K. A., Rajagopalan, P. T. R., Benkovic, S. J., and Kohen, A. (2004) Tuneling and coupled motion in the *E. coli* dihydrofolate reducatse catalysis. *J. Am. Chem. Soc. 126*, 4778−4779.

(13) Knapp, M. J., and Klinman, J. P. (2002) Environmentally coupled hydrogen tunneling - Linking catalysis to dynamics. *Eur. J. Biochem. 269*, 3113−3121.

(14) Klinman, J. P. (2009) An integrated model for enzyme catalysis emerges from studies of hydrogen tunneling. *Chem. Phys. Lett. 471*, 179−193.

(15) Wang, L., Goodey, N. M., Benkovic, S. J., and Kohen, A. (2006) Coordinated effects of distal mutations on environmentally coupled

tunneling in dihydrofolate reductase. *Proc. Natl. Acad. Sci. U.S.A. 103*, 15753−15758.
(16) Hvidt, A. (1964) A Discussion of the pH dependence of the hydrogen-deuterium exchange of proteins. *Cr. Trav. Lab. Carlsberg 34*, 299−317.
(17) Swint-Kruse, L., and Robertson, A. D. (1996) Temperature and pH dependences of hydrogen exchange and global stability for ovomucoid third domain. *Biochemistry 35*, 171−180.
(18) Oyeyemi, O.A., Sours, K. M., Lee, T., Resing, K. A., Ahn, N. G., and Klinman, J. P. (2010) Temperature dependence of protein motions in a thermophilic dihydrofolate reductase and its relationship to catalytic efficiency. *Proc. Natl. Acad. Sci. U.S.A. 107*, 10074−10079.
(19) Andreotti, G., Cubellis, M. V., Palo, M. D., Fessas, D., Sannia, G., and Marino, G. (1997) Stability of a thermophilic TIM-barrel enzyme: indole-3-glycerol phosphate synthase from the thermophilic archaeon *Sulfolobus solfataricus*. *Biochem. J. 323* (Pt 1), 259−264.
(20) Sriprapundh, D. (2003) Directed evolution of *Thermotoga neapolitana* xylose isomerase: high activity on glucose at low temperature and low pH. *Protein Eng. 16*, 683−690.
(21) Wintrode, P. L., Zhang, D. Q., Vaidehi, N., Arnold, F. H., and Goddard, W. A. (2003) Protein dynamics in a family of laboratory evolved thermophilic enzymes. *J. Mol. Biol. 327*, 745−757.
(22) Arnold, F. H., Giver, L., Gershenson, A., Zhao, H., and Miyazaki, K. (1999) Directed evolution of mesophilic enzymes into their thermophilic counterparts. *Ann. N.Y. Acad. Sci. 870*, 400−403.
(23) Spiller, B., Gershenson, A., Arnold, F. H., and Stevens, R. C. (1999) A structural view of evolutionary divergence. *Proc. Natl. Acad. Sci. U.S.A. 96*, 12305−12310.
(24) Giver, L., Gershenson, A., Freskgard, P. O., and Arnold, F. H. (1998) Directed evolution of a thermostable esterase. *Proc. Natl. Acad. Sci. U.S.A. 95*, 12809−12813.
(25) Somero, G.N. (1978) Temperature adaptation of enzymes - biological optimization through structure-function compromises. *Ann. Rev. Ecol. Syst. 9*, 1−29.
(26) Blakley, R. L. (1960) Crystalline dihydropteroylglutamic acid. *Nature 188*, 231−232.
(27) Sours, K. M., Kwok, S. C., Rachidi, T., Lee, T., Ring, A., Hoofnagle, A. N., Resing, K. A., and Ahn, N. G. (2008) Hydrogen-exchange mass spectrometry reveals activation-induced changes in the conformational mobility of p38 alpha MAP kinase. *J. Mol. Biol. 379*, 1075−1093.
(28) Resing, K. A., Hoofnagle, A. N., and Ahn, N. G. (1999) Modeling deuterium exchange behavior of ERK2 using pepsin mapping to probe secondary structure. *J. Am. Soc. Mass. Spectrom. 10*, 685−702.
(29) Hoofnagle, A. N., Resing, K. A., and Ahn, N. G. (2003) Protein analysis by hydrogen exchange mass spectrometry. *Annu. Rev. Biophys. Biomol. Struct. 32*, 1−25.
(30) Bai, Y., Milne, J. S., Mayne, L., and Englander, S. W. (1993) Primary structure effects on peptide group hydrogen exchange. *Proteins 17*, 75−86.
(31) Xu, D., and Zhang, Y. (2009) Generating triangulated macromolecular surfaces by Euclidean Distance Transform. *PLoS One 4*, e8140.
(32) Yamamoto, T., Izumi, S., and Gekko, K. (2004) Mass spectrometry on segment-specific hydrogen exchange of dihydrofolate reductase. *J. Biochem. (Tokyo) 135*, 17−24.
(33) Liu, Y. H., and Konermann, L. (2006) Enzyme conformational dynamics during catalysis and in the 'resting state' monitored by hydrogen/deuterium exchange mass spectrometry. *FEBS Lett. 580*, 5137−5142.
(34) Schnell, J. R., Dyson, H. J., and Wright, P. E. (2004) Structure, dynamics, and catalytic function of dihydrofolate reductase. *Annu. Rev. Biophys. Biomol. Struct. 33*, 119−140.
(35) Bhabha, G., Lee, J., Ekiert, D. C., Gam, J., Wilson, I. A., Dyson, H. J., Benkovic, S. J., and Wright, P. E. (2011) A dynamic knockout reveals that conformational fluctuations influence the chemical step of enzyme catalysis. *Science 332*, 234−238.
(36) Liang, Z.-X., Tsigos, I., Lee, T., Bouriotis, V., Resing, K. A., Ahn, N. G., and Klinman, J. P. (2004) Evidence for increased local flexibility in psychrophilic alcohol dehydrogenase relative to its thermophilic homologue. *Biochemistry 43*, 14676−14683.